Article

Structural Evolution of the Pharmaceutical Peptide Octreotide upon Controlled Relative Humidity and Temperature Variation

Maria Athanasiadou [1], Christina Papaefthymiou [1], Angelos Kontarinis [1], Maria Spiliopoulou [1], Dimitrios Koutoulas [1], Marios Konstantopoulos [1], Stamatina Kafetzi [1], Kleomenis Barlos [2], Kostas K. Barlos [2], Natalia Dadivanyan [3], Detlef Beckers [3], Thomas Degen [3], Andrew N. Fitch [4] and Irene Margiolaki [1,*]

[1] Department of Biology, Section of Genetics, Cell Biology and Development, University of Patras, 26500 Patras, Greece; mariaath9888@gmail.com (M.A.)
[2] CBL-Patras, Patras Industrial Area, Block 1,25018 Patras, Greece; barlos@cblpatras.gr (K.B.); kostas.barlos@cblpatras.gr (K.K.B.)
[3] Malvern Panalytical B.V., Lelyweg 1, 7602 EA Almelo, The Netherlands
[4] European Synchrotron Radiation Facility, CS40220, 38043 Grenoble Cedex 9, Rhône-Alpes, France
* Correspondence: imargiola@upatras.gr

Abstract: Octreotide is the first synthetic peptide hormone, consisting of eight amino acids, that mimics the activity of somatostatin, a natural hormone in the body. During the past decades, advanced instrumentation and crystallographic software have established X-Ray Powder Diffraction (XRPD) as a valuable tool for extracting structural information from biological macromolecules. The latter was demonstrated by the successful structural determination of octreotide at a remarkably high d-spacing resolution (1.87 Å) (PDB code: 6vc1). This study focuses on the response of octreotide to different humidity levels and temperatures, with a particular focus on the stability of the polycrystalline sample. XRPD measurements were accomplished employing an Anton Paar MHC-trans humidity-temperature chamber installed within a laboratory X'Pert Pro diffractometer (Malvern Panalytical). The chamber is employed to control and maintain precise humidity and temperature levels of samples during XRPD data collection. Pawley analysis of the collected data sets revealed that the octreotide polycrystalline sample is remarkably stable, and no structural transitions were observed. The compound retains its orthorhombic symmetry (space group: $P2_12_12_1$, a = 18.57744(4) Å, b = 30.17338(6) Å, c = 39.70590(9) Å, d ~ 2.35 Å). However, a characteristic structural evolution in terms of lattice parameters and volume of the unit cell is reported mainly upon controlled relative humidity variation. In addition, an improvement in the signal-to-noise ratio in the XRPD data under a cycle of dehydration/rehydration is reported. These results underline the importance of considering the impact of environmental factors, such as humidity and temperature, in the context of structure-based drug design, thereby contributing to the development of more effective and stable pharmaceutical products.

Keywords: humidity variation; temperature variation; X-ray crystallography; peptides; polymorphism; octreotide; drug stability; in situ X-Ray Powder Diffraction

1. Introduction

Structural biology plays a pivotal role in advancing the understanding of biological structures and functions, offering invaluable insights into the molecular intricacies that underlie life processes. Crystallization and the preservation of peptide and protein crystallinity represent a subtle interplay, where the interaction of various factors can significantly impact the outcome [1–3]. Among these factors, environmental conditions emerge as critical factors, with relative humidity (rH) and temperature standing out. The balance between hydration and dehydration can influence crystal size, morphology, and diffraction quality [4,5]. Moreover, the water content within macromolecular crystals can impact the conformational stability of the molecules, adding an extra layer of complexity to the

relationship between rH and crystal structure. Temperature is another important variable, as temperature fluctuations can affect the thermal motion of atoms within the crystal lattice, potentially impacting the integrity of the crystalline order [6–8]. Insights from this type of research not only have implications for fundamental biological understanding but also hold promise for the development of novel therapeutics and biotechnological applications, as peptide and protein crystals, with their advantages, are increasingly utilized in creating drug carriers and excipients that exhibit prolonged action and improved physicochemical properties, allowing for the modification of the drug's performance properties.

1.1. Structural Characterization of Peptide-Based Drugs via X-ray Powder Diffraction (XRPD)

In the framework of assessing the stability of polycrystalline peptide-based pharmaceuticals, X-ray Powder Diffraction (XRPD) is the most appropriate method for gaining insights into the crystalline integrity of a molecule. This involves the identification of potential polymorphisms and the detection of conformational alterations at the unit-cell level [9–14]. Stability studies aim to establish optimal storage conditions for a drug substance, incorporating tests for thermal stability and, if relevant, sensitivity to moisture. Consequently, conducting in situ XRPD measurements under controlled temperature and humidity conditions emerges as a potent tool for studying structural modifications of biological macromolecules. In general, temperature variations can induce polymorphic transitions or degradation, while the sorption and desorption of water can alter the structure and properties of a substance [5,6,15–19]. The synergistic implementation of XRPD and a humidity-temperature chamber enables real-time observation of structural adaptation through controlled changes. This approach, involving the evaluation of diffraction patterns and their subsequent analysis, leads to important conclusions about the structural evolution of the molecule.

1.2. The Pharmaceutical Peptide Octreotide

In recent years, peptides have emerged as a distinctive class of therapeutic agents due to their unique biochemical characteristics and therapeutic potential. While the initial focus on therapeutic peptides was centered on mimicking natural hormones, the trends in discovery and development have evolved. To date, there has been a shift from merely replicating hormones or peptides derived from nature to the rational design of peptides with specific and desirable biochemical and physiological activities. This evolution has been facilitated by significant advances in structural chemistry and biology, and the production of polycrystalline drugs is increasingly desirable [20].

In this study, the polycrystalline sample of octreotide, an eight-amino-acid peptide, and the initial synthetic analogue of somatostatin (SS) are investigated thoroughly. Octreotide is currently commercially available as a suspension of amorphous counterparts, suitable for subcutaneous or intravenous injection in the management and treatment of diseases such as acromegaly and thyrotrophinomas [21–23]. However, there is a prominent interest in investigating the microcrystalline form of the product. The latter could potentially offer improved absorption, distribution, metabolism, and excretion (ADME) characteristics, along with prolonged action and stability.

Building upon the successful crystallization and structural characterization of the peptide achieved a few years ago using high-resolution synchrotron XRPD data [21,23], this study aims to further explore the stability of the polycrystalline form upon variation of its environmental conditions. While previous studies have investigated the stability of octreotide in sterile solution under controlled conditions, including storage at temperatures of 2–8 °C for 24 months and elevated conditions of 25 °C/60% rH [24], the in situ real-time study of the crystalline precipitate has not been previously reported. This presents an intriguing opportunity to explore the adaptation of octreotide in its crystalline form under varying environmental conditions. The main objective is to comprehensively characterize its potential as an enhanced pharmaceutical formulation, reinforcing the proposal for crystalline drugs for this peptide. Simultaneously, this study demonstrates the feasibility

of such investigations in biological molecules as part of Structure-Based Drug Design (SBDD) [25].

1.3. In Situ XRPD Measurements upon Controlled Relative Humidity and Temperature Variation

To successfully conduct the targeted experiments, precise control of both rH and temperature was crucial. For this purpose, the MHC-trans humidity-temperature chamber (Multi-sample Humidity Chamber TRANsmission) from Anton Paar (Graz, Austria) was installed within the laboratory X'Pert Pro diffractometer (Malvern Panalytical, Almelo, the Netherlands). This chamber is well-suited for conducting in situ XRPD measurements, enabling the observation of structural changes under carefully controlled temperature and humidity conditions. The system employs two interconnected control units to manage sample temperature and rH, ensuring accuracy while preventing condensation. The chamber accommodates up to 8 samples simultaneously, maintaining uniform conditions and allowing each sample to be positioned in the X-ray beam for XRPD data collection. This setup is not only time-efficient but also ensures accurate data collection while preserving optimal experimental conditions, and it is the most suitable for the stress testing of substances [18,19].

1.4. Advances of the Current Study

Previous studies have extensively investigated various aspects of octreotide, including its biochemical properties, therapeutic applications, and structural characteristics. Research has focused on elucidating octreotide's role in managing conditions such as acromegaly, carcinoid syndrome, and neuroendocrine tumors, shedding light on its clinical benefits and limitations [26–28]. Additionally, studies have delved into octreotide's pharmacokinetic profile, encompassing aspects such as ADME characteristics essential for optimizing dosing regimens and predicting therapeutic outcomes [29–31]. Furthermore, formulation strategies for octreotide have been explored to enhance its stability, bioavailability, and duration of action through novel delivery systems and formulations [32–34]. Notably, oral capsules have been developed to enable the oral delivery of octreotide, demonstrating promising stability and desired bioavailability in preclinical and clinical studies [24]. Structural characterization studies using techniques such as X-ray crystallography and XRPD have provided insights into the molecular structure of octreotide, elucidating their stability and microcrystalline formulation behavior [21–23].

Despite these advancements, gaps persist in understanding the impact of environmental factors, such as rH and temperature, on octreotide's stability and structural integrity. This study aims to address these challenges by investigating the structural behavior of octreotide under controlled rH and temperature conditions, employing high-resolution synchrotron XRPD coupled with in situ laboratory XRPD measurements. By employing advanced experimental methods, this research provides insights into the dynamic response of the microcrystalline compound to variations in its environmental conditions.

Moreover, while oral capsules represent a significant advancement in delivering octreotide orally, there is potential for further improvement through crystalline formulation. Crystalline formulations offer the possibility of enhanced stability and structural integrity compared to conventional oral capsules, something that is highlighted by the remarkable resilience of octreotide presented in this study. Furthermore, by demonstrating the feasibility of in situ XRPD measurements for studying structural modifications in biological molecules, this study expands the methodological toolkit available for SBDD.

2. Results

Following the crystallization of octreotide, the orthorhombic symmetry (space group $P2_12_12_1$) was identified via XRPD data collection in capillary mode employing the laboratory diffractometer X'Pert Pro (Malvern Panalytical) and the ESRF beamline ID22. No intermixture of crystalline phases was observed. Pawley analysis of the laboratory XRPD data yielded satisfactory results (Figure 1) [space group: $P2_12_12_1$, a = 18.608(2) Å,

b = 30.254(3) Å, c = 39.794(6) Å] with typical agreement factors of R_{wp} = 4.8158% and χ^2 = 2.161. Pawley analysis of the synchrotron data was satisfactory, providing precise lattice parameters [a = 18.57744(4) Å, b = 30.17338(6) Å, c = 39.70590(9) Å] and typical agreement factors of R_{wp} = 5.39% and χ^2 = 1.29 (Figure 2). The data acquired for the octreotide polycrystalline samples extended to an enhanced d-spacing resolution of approximately 2.35 Å.
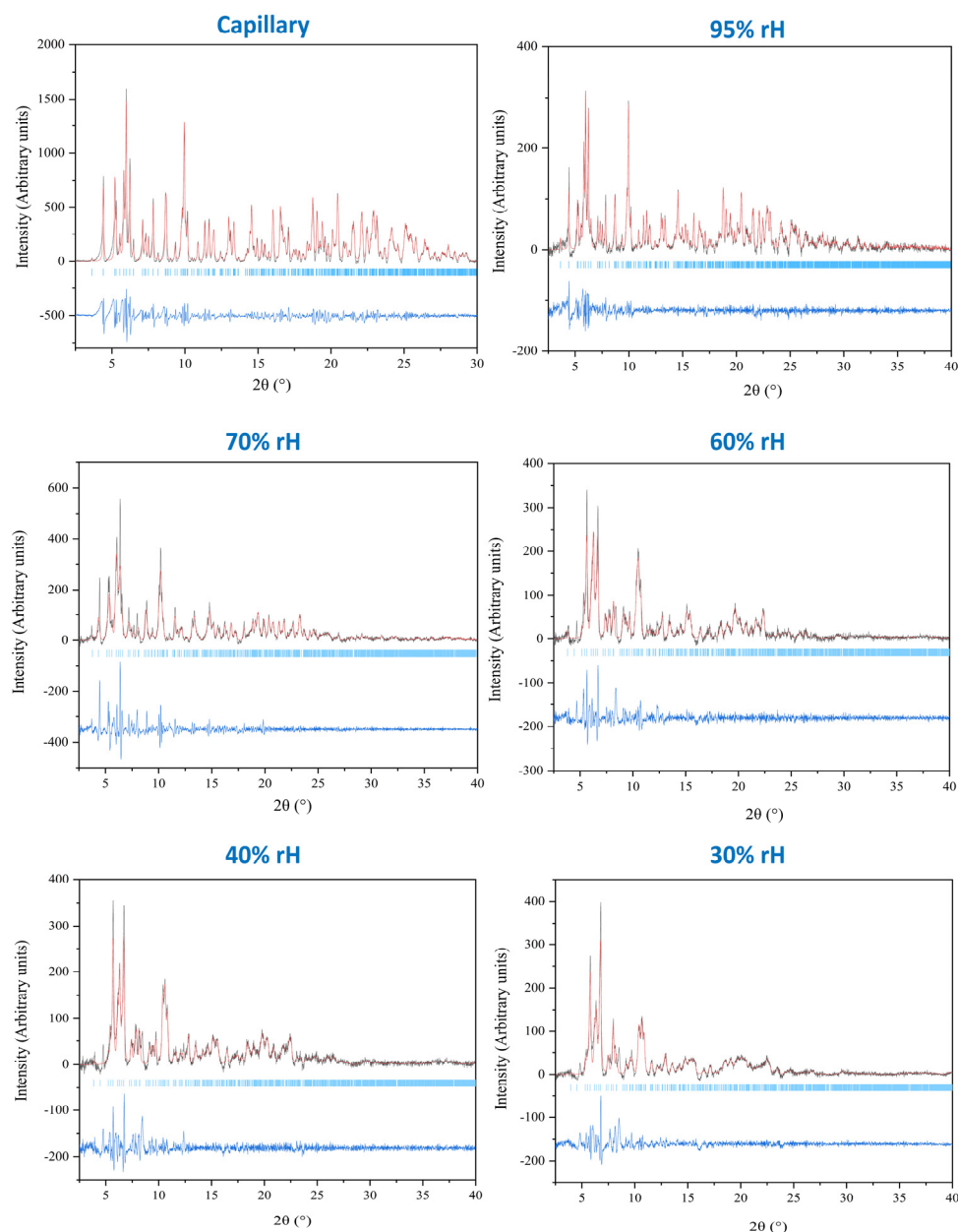

Figure 1. Pawley fits of XRPD data of polycrystalline octreotide at ambient conditions (capillary mode) and selected rH levels (95%, 70%, 60%, 40%, and 30%). The data extend up to ~2.35 Å resolution. They were collected employing a laboratory X-ray powder diffractometer (X'Pert Pro, Malvern Panalytical) equipped with an Anton Paar MHC-trans humidity-temperature chamber [λ = 1.540598 Å, RT]. In each panel, the black and red lines represent the experimental data and the calculated profiles, respectively, while the blue line corresponds to the difference between the experimental and calculated profiles. The vertical bars indicate the Bragg reflections compatible with this space group ($P2_12_12_1$, lattice parameters at ambient conditions: a = 18.608(2) Å, b = 30.254(3) Å, and c = 39.794(6) Å).
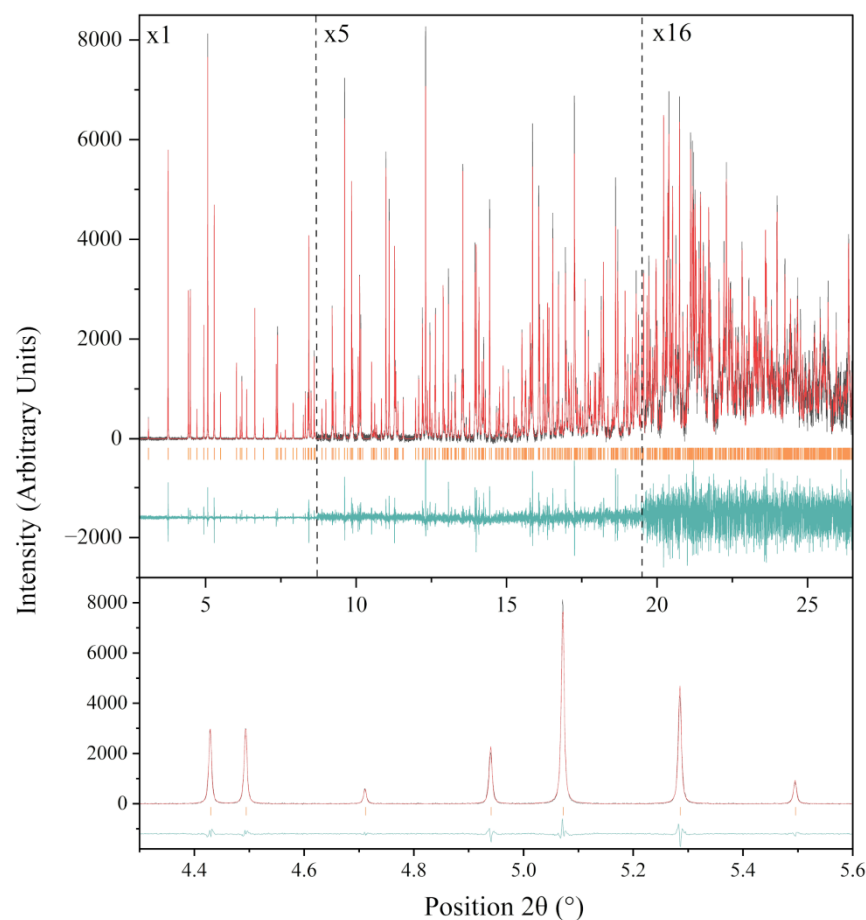
Figure 2. Upper panel: Pawley fit of the XRPD synchrotron data of octreotide. The data were collected on ID22 at ESRF and extend up to ~2.35 Å resolution [λ = 1.3007899(8) Å, RT]. The black, red, and lower green lines represent the experimental data, the calculated pattern, and the difference between the experimental and calculated profiles, respectively. The orange vertical bars correspond to Bragg reflections compatible with this space group ($P2_12_12_1$, a = 18.57744(4) Å, b = 30.17338(6) Å, and c = 39.70590(9) Å). To highlight the enhanced d-spacing resolution, the profile was systematically multiplied by factors of 5 and 16, as indicated in the figure. Lower panel: Magnification of the 2θ range from 4.3° to 5.6°, emphasizing the enhanced angular resolution of the diffraction pattern. The background intensity has been subtracted for clarity.

Data analysis of the diffraction patterns at all rH and temperature levels revealed the stability of the orthorhombic crystal symmetry, and there was no phase transition even at the lowest rH level of 30%, at which unit-cell parameters were determined via Pawley analysis [a = 18.66(1), b = 28.21(2), c = 39.78(3) Å] and agreement factors of R_{wp} = 2.095% and χ^2 = 2.48697.

2.1. The Effect of rH Variation on Octreotide at Ambient Temperature

Data analysis unveiled a distinct evolution of the unit cell during subsequent dehydration and rehydration processes, as evidenced by the surface plots of the XRPD patterns, depicting a consistent modification in diffraction peak positions (Figure 3). It is noteworthy that despite the dehydration process, minimal shifts of the diffraction peaks to lower angles were observed, indicating subtle variation of the unit-cell parameters, which are reversible upon rehydration. Specifically, during gradual dehydration, the orthorhombic a and c axes progressively increase by an absolute value of 0.51% and 0.27%, respectively, in the cycle with a lower relative humidity (rH) level of 30%, while the b axis significantly decreases by an absolute value of 6.43% (Figure 4). Detailed values of the modifications to unit-cell parameters for each experimental cycle are provided in Table 1. At an rH level of <75%,

a sudden modification in the unit cell occurs (Figure 5), particularly evident in the b axis, which rapidly decreases (Figure 4).
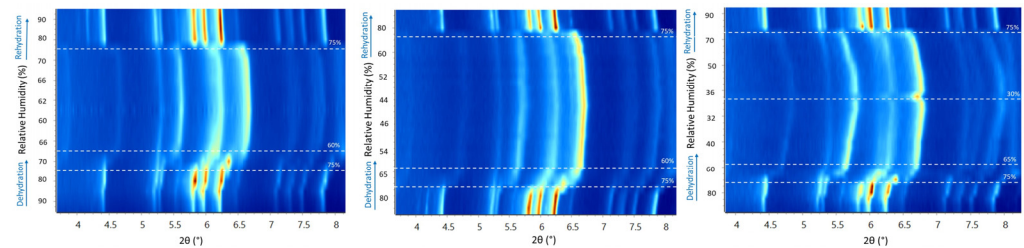

Figure 3. Surface plots of laboratory XRPD data of the octreotide polycrystalline precipitate upon gradual dehydration/rehydration cycles from 95% to 60% rH (**left**), 95% to 40% rH (**middle**), and 95% to 30% (**right**). Alterations of the peak positions and intensities are evident upon gradual dehydration and rehydration cycles. Significant peak shifts become evident upon dehydration, particularly below 70% rH. Upon rehydration and above 75% rH, the sample effectively recovers to its initial state.
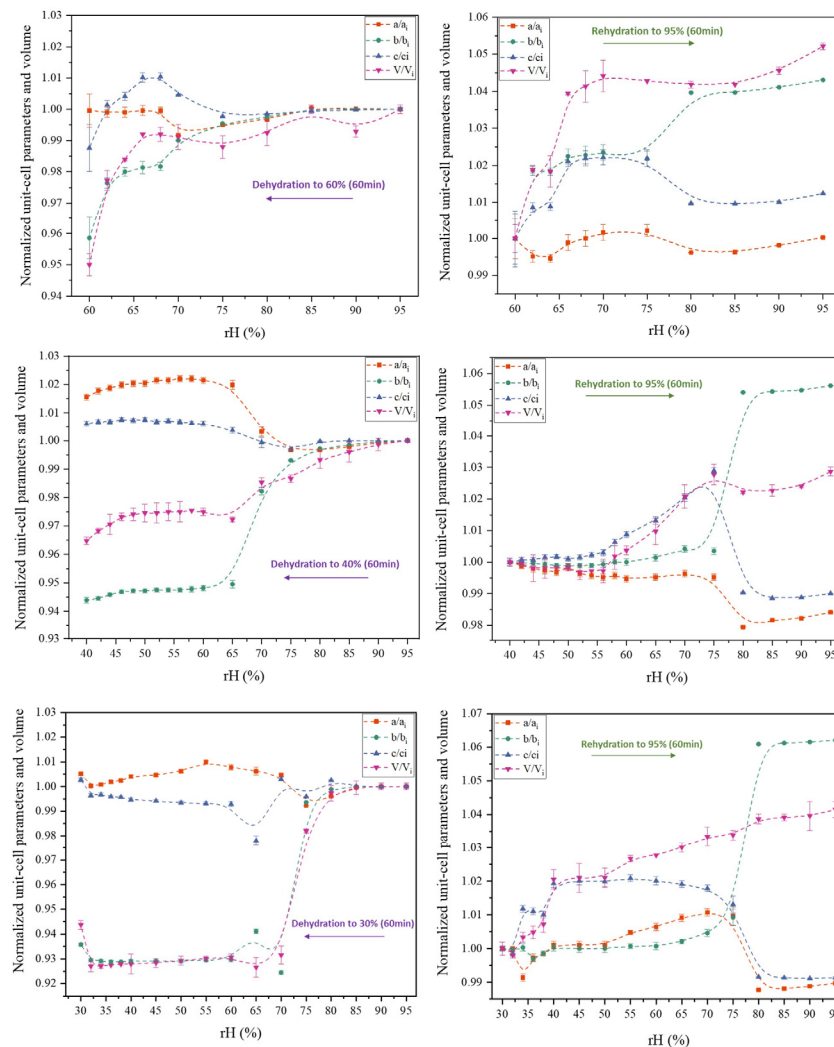

Figure 4. Evolution of normalized unit-cell parameters upon gradual dehydration and rehydration of the octreotide polycrystalline sample from 95% to 60% rH (**upper panel**), 40% rH (**middle panel**), and 30% rH (**lower panel**). Purple, red, green, and blue symbols correspond to the extracted parameters of the unit-cell volume V, the a axis, the b axis, and the c axis, respectively. The lines are guides to the eye.

Table 1. Modifications of unit-cell parameters of octreotide upon gradual dehydration. Delta variations were calculated as $\Delta(x_i - x_f)/x_i$ % between the initial (x_i) and final (x_f) values, extracted for the orthorhombic polymorph.

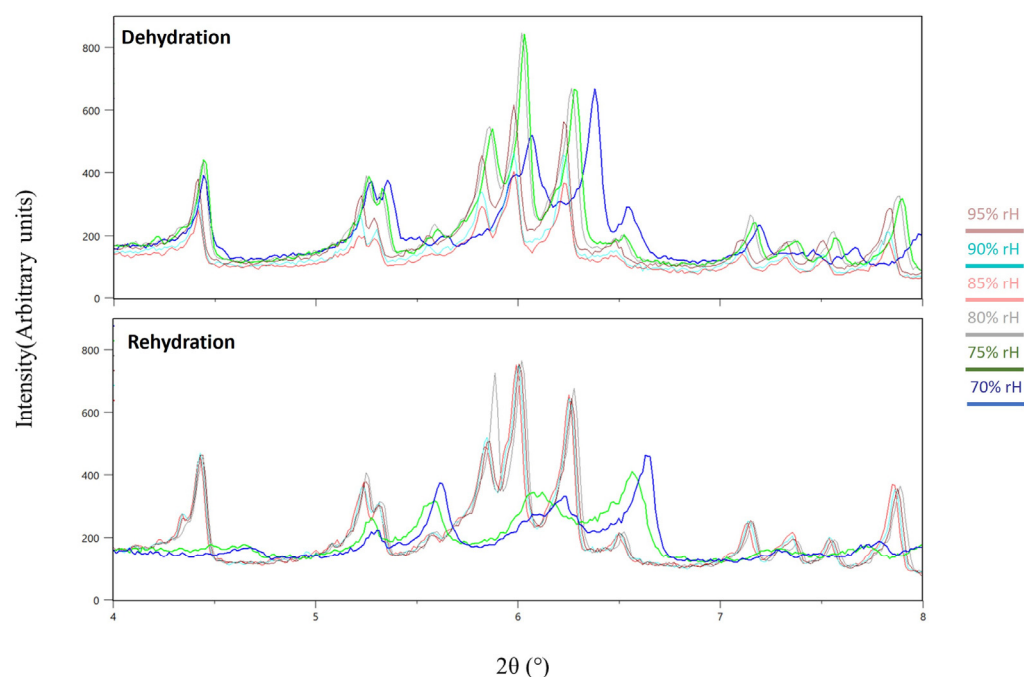|	95–60% rH	95–40% rH	95–30% rH
$\Delta a/a_i$ (%)	0.04	-1.56	-0.51
$\Delta b/b_i$ (%)	4.14	5.61	6.43
$\Delta c/c_i$ (%)	1.24	-0.61	-0.27
$\Delta V/V_i$ (%)	5.00	3.53	5.63

Figure 5. Magnification of the laboratory XRPD data in the 4–8° 2*θ* range reveals significant peak shifts at 75% and 70% rH (RT), along with the subsequent recovery of the sample after rehydration.

Throughout this process, crystallinity is maintained, and upon subsequent rehydration, the sample recovers to its initial state. Notably, data quality improves in terms of signal-to-noise ratio under a cycle of dehydration/rehydration (Figure 6). The 60-min waiting time interval appears satisfactory for sample adaptation.

2.2. The Effect of Temperature on Octreotide at Selected rH Levels

Surface plots of XRPD data of octreotide upon temperature variation at the selected humidity levels of 95%, 85%, 75%, 65%, 55%, and 45% reveal the absence of considerable diffraction peak shifts at 95% and 85% rH (Figure 7). This observation is evident for both the heating and cooling processes between 294.15 K and 318.15 K. At 75% and 65% rH, subtle peak shifts and intensity modifications are observed. However, with respect to the results obtained upon rH variation at ambient temperature, it is apparent that temperature has a less pronounced effect on the unit-cell dimensions. In this case, the evolution of the unit-cell parameters (Figure 8) indicates that the a, b, and c axes remain relatively stable, except for the 75% and 65% rH levels, where there is a noticeable decrease primarily in the b and c axes, by an absolute value of 7.30% and 2.57%, respectively, observed at 65% rH (Table 2). These specific rH levels appear critical for the changes in peak positions and the subtle modifications observed in the diffraction patterns.
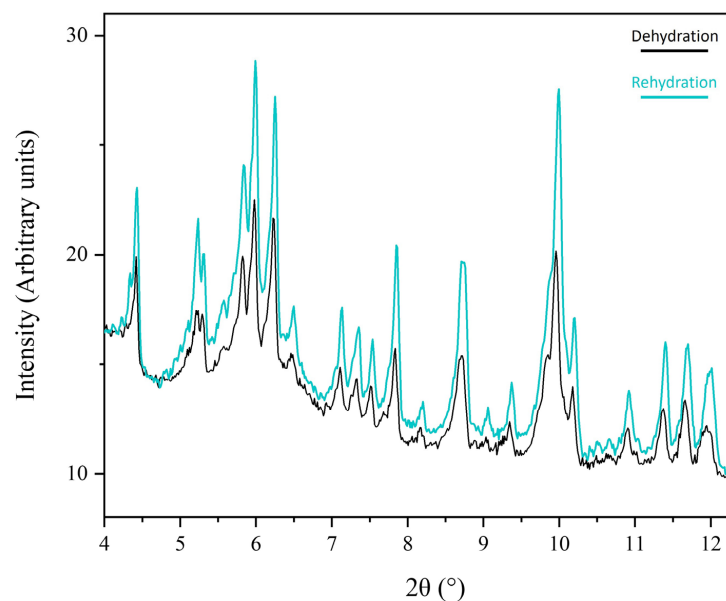
Figure 6. Following a complete dehydration and rehydration cycle, a comparative view of XRPD data at 95% rH reveals a pronounced improvement of the XRPD data in terms of signal-to-noise ratio.
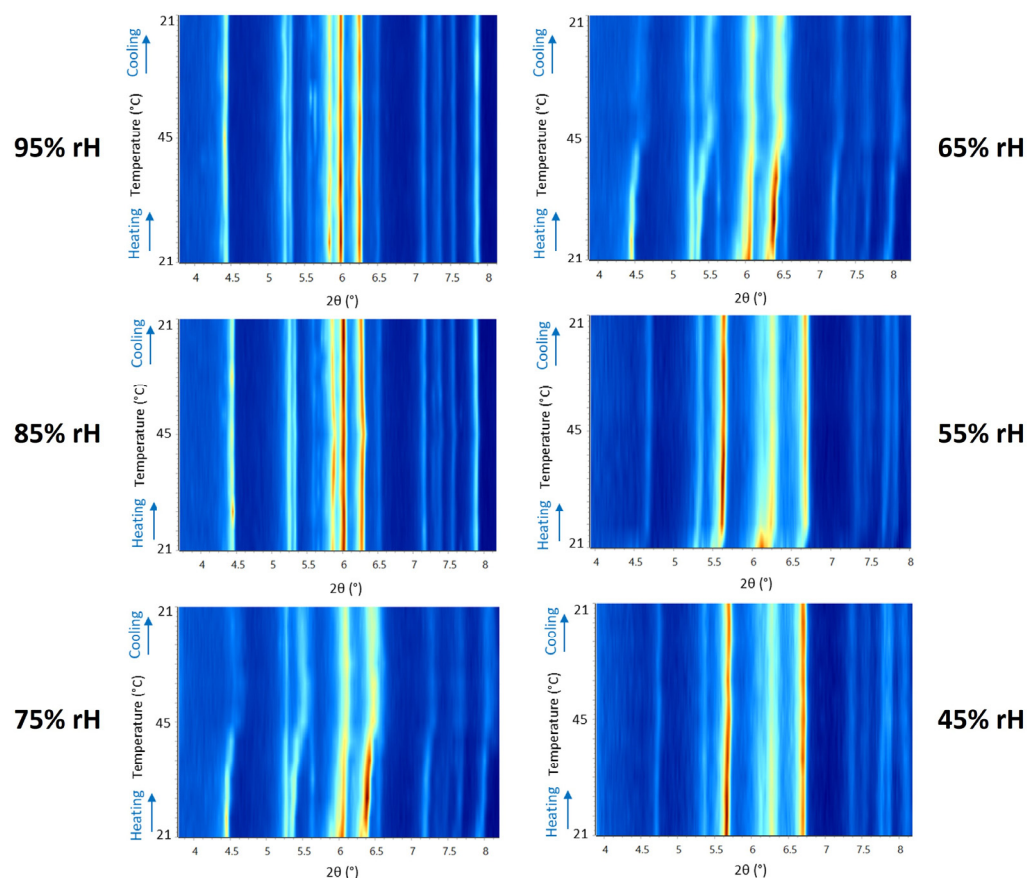

Figure 7. Surface plots of XRPD data of octreotide polycrystalline precipitate upon gradual heating/cooling cycles at specific rH levels. A noticeable shift in the diffraction peak positions and intensities is observed at 75% and 65% rH. The latter observation may be attributed more to the effect of humidity than temperature. In addition, the XRPD data collected upon rH variation at ambient temperature described above indicate that at rH lower than 75%, the sample exhibits a slight alteration in terms of unit-cell dimensions, yet crystallinity is maintained. The latter suggests that temperature does not significantly impact the structural integrity of the polycrystalline peptide sample.
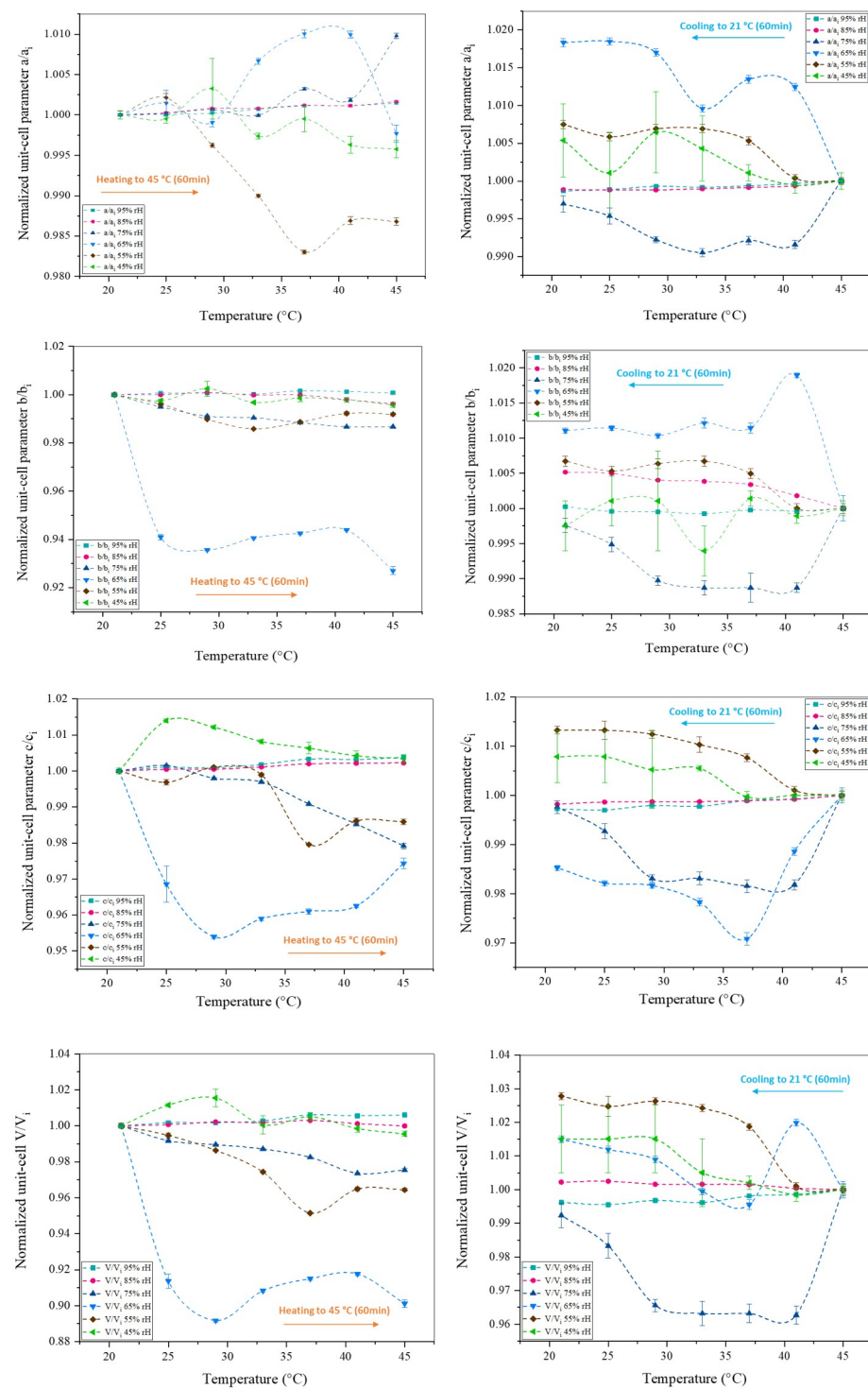
Figure 8. Evolution of normalized unit-cell parameters upon gradual heating and cooling cycles of the octreotide polycrystalline sample from 294.15 K to 318.15 K at selected rH levels. Turquoise, pink, dark blue, light blue, brown, and green symbols correspond to the rH levels of 95%, 85%, 75%, 65%, 55%, and 45%, respectively. The lines are guides to the eye.

In summary, the results described above indicate that the crystal structure is significantly affected by gradual dehydration, while it is a reversible process upon rehydration to the initial rH level of 95% (Figure 4, Table 1). Temperature variation has a minor effect on the crystal structure with respect to rH (Figure 8, Table 2). The diffraction signal remains satisfying at all conditions, indicating that the samples retain their crystallinity. The crystal

structure is stable with a 60-min waiting time interval to adapt to each condition, which suggests that the system reaches an equilibrium state.

Table 2. Modifications of unit-cell parameters of octreotide upon gradual heating in each of the selected rH levels. Delta variations were calculated as $\Delta(x_i - x_f)/x_i$ % between the initial (x_i) and final (x_f) values, extracted for the orthorhombic polymorph.

294.15–318.15 K	95% rH	85% rH	75% rH	65% rH	55% rH	45% rH
$\Delta a/a_i$ (%)	−0.15	−0.16	−0.98	0.23	1.32	0.42
$\Delta b/b_i$ (%)	−0.08	0.38	1.33	7.30	0.81	0.42
$\Delta c/c_i$ (%)	−0.38	−0.22	2.08	2.57	1.41	−0.34
$\Delta V/V_i$ (%)	−0.61	0.00	2.46	9.89	3.56	0.45

3. Materials and Methods

3.1. Crystallization

The octreotide peptide, supplied in the form of a lyophilized acetate salt powder by the pharmaceutical company CBL Patras (Patras, Greece), underwent the crystallization procedure using the evaporation method reported earlier [21–23]. In particular, samples with a concentration of 217 mg mL^{-1} were produced via the dilution of octreotide acetate powder in 0.2 M oxalic acid. The dilution process took place directly within the wells of a 24-well crystallization plate, which was subsequently sealed with Parafilm to prevent sample dehydration. Two to three pinholes were carefully created in the film to facilitate gradual evaporation. The plate underwent incubation at 322.95 K with stirring at 120 rpm until the complete dilution of octreotide powder in the solvent. Subsequently, the stirring rate was reduced to 80 rpm until the solvent was nearly evaporated. Each sample was then re-dissolved in 95 μL of ddH$_2$O and incubated at 298 K without stirring until almost complete water evaporation. This final step was repeated several times using 47.5 μL of ddH$_2$O until a white precipitate became visible. Following this, the samples were preserved using 47.5 μL of ddH$_2$O until no further increase in precipitate was observed. After each step, the wells were resealed with Parafilm, and pinholes were reintroduced. The resulting precipitate from each sample was transferred to an Eppendorf tube, where 250 μL of ddH$_2$O was added before storage at 298 K. Samples were kept sealed in Eppendorf tubes and stored at RT prior to XRPD measurements. To verify the crystallinity of the produced precipitate, observation under optical microscopy was conducted (Figure 9).
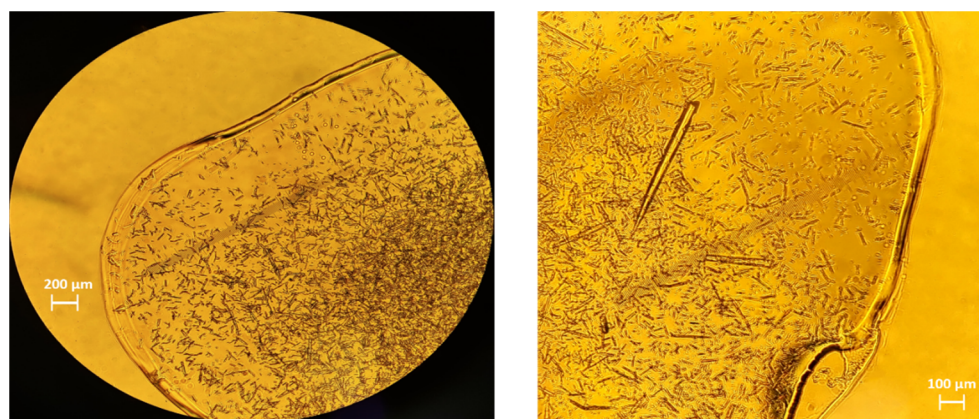

Figure 9. Optical microscopy images of the polycrystalline octreotide sample.

3.2. Laboratory and Synchrotron XRPD Data Collection

Laboratory XRPD data were initially collected using a laboratory X'Pert Pro diffractometer (Malvern Panalytical, Almelo, The Netherlands) with focusing *Kα* geometry to measure samples loaded into 1.0 mm diameter borosilicate glass capillaries and identify the

presence of the orthorhombic symmetry of the octreotide crystals (space group: $P2_12_12_1$, a = 18.608(2) Å, b = 30.254(3) Å, c = 39.794(6) Å). On the incident-beam side, a focusing X-ray mirror for Cu radiation (λ = 1.540598 Å) was paired with a 0.5° anti-scatter slit, a 0.04 rad Soller slit, a 10 mm mask, and a 1/2° divergence slit. On the diffracted-beam side, the configuration included a 0.04 rad Soller slit and a PIXcel^{1D} detector with anti-scatter shielding. 2θ scans were initiated with a starting angle of 0°, which was possible without any harm to the detector due to a beam-stop mounted on the anti-scatter device of the X-ray mirror.

In order to extract more accurate unit-cell dimensions, data with enhanced angular resolution were collected under ambient conditions at the high-resolution powder diffraction beamline, ID22 [λ = 1.3007899(8) Å, RT] [35], of the European Synchrotron Radiation Facility (ESRF) in Grenoble. All samples were loaded into 1.0 mm diameter borosilicate glass capillaries and centrifuged in order to enhance crystal packing. Excess mother liquor was removed, and the capillaries were sealed with silicone vacuum grease to prevent dehydration. The capillaries were affixed to the diffractometer and rotated at a speed of 1031 revolutions per minute to ensure sufficient powder averaging. The process involved the utilization of an automated sample-changing robot for both loading and unloading the samples. This was achieved by placing the capillaries into self-centering magnetic bases. Multiple scans were collected for each sample position, and the capillaries were periodically translated axially to expose new sections of the sample that had not been affected by the synchrotron beam. The effects of radiation damage were observed through noticeable changes in unit-cell parameters, a decrease in the diffraction signal, and gradual peak broadening [10,35,36]. These effects could be tracked by comparing the profiles measured in each of the thirteen detector channels during a single scan as well as across subsequent scans. The initial scans, taken right after the sample was translated to expose fresh material, were combined with the scans of each sample position that did not exhibit detectable degradation to enhance counting statistics, whereas the rest were mainly used to monitor the changes in unit-cell parameters with increasing sample exposure time to the X-ray beam. The collected patterns were typically indexed using the HighScore Plus software [37] and the fitted positions of at least the first twenty reflections of the XRPD profiles. In order to extract accurate unit-cell parameter values and to analyze peak shape and background coefficients without the use of a structural model, Pawley refinement [38] processes were performed to verify the orthorhombic symmetry (space group: $P2_12_12_1$, a = 18.57744(4) Å, b = 30.17338(6) Å, c = 39.70590(9) Å).

In situ laboratory XRPD data were collected using the transmission temperature and humidity chamber MHC-trans (Anton Paar, Graz, Austria). In this case, an elliptical focusing X-ray mirror for Cu radiation (λ = 1.540598 Å) was used on the incident-beam side with a 1/4° divergence slit (~1mm thickness), 0.04 rad Soller slits, and a 1/4° anti-scatter slit. On the diffracted-beam side, a PIXcel^{1D} detector was employed with a 7.5 mm anti-scatter slit and a Soller slit of 0.04°. The detector was used in one-dimensional data-collection mode. The low 2θ angle part of the diffraction profile generally contains the strongest reflections. The slits were used to reduce the scattering close to the direct beam, enhancing the signal-to-noise ratio. 2θ scans were performed within a range of 2–30°.

Protein crystalline precipitates stored in Eppendorf tubes were centrifuged, and excess mother liquor was removed. Polycrystalline specimens for in situ XRPD measurements were loaded into thin Kapton-foil holders in order to reduce background contribution and were placed on a multiple position sample holder (Figure 10). Excess mother liquor was removed, and samples were sealed with silicone vacuum grease to prevent dehydration.
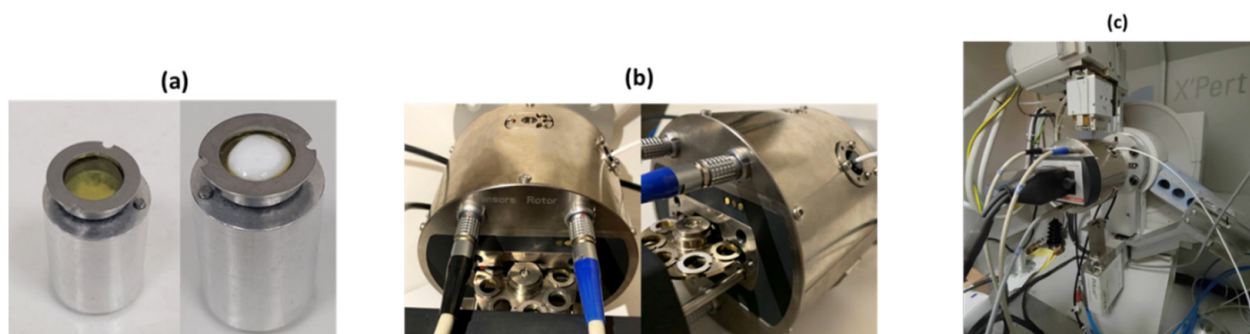
Figure 10. (**a**) Empty Kapton foil holder (**left**) and Kapton foil holder filled with the polycrystalline octreotide sample (**right**). (**b**) View of the interior of the humidity chamber containing the multiple-position sample holder. (**c**) The configuration of the X'Pert Pro diffractometer equipped with the MHC-trans humidity and temperature chamber for in situ XRPD data collection in transmission mode.

In order to examine the structural modifications in the polycrystalline samples upon rH and temperature variation as well as the effect of the variation rate on that process, different cycles of experiments were conducted following different approaches. A total of 3 cycles of XRPD data collection were performed to study the response of the peptide to varying rH levels via subsequent dehydration and rehydration processes. The aim was to test the peptide's resilience within a rH range of 95% to 30% at a constant temperature of 294.15 K. Each step involved a 60-min waiting time before collecting each scan to allow for the sample to equilibrate. For each rH level, 10 scans were collected, with each scan lasting approximately 2 min. To obtain a more detailed understanding of changes across a broad range of rH levels, specific steps of transition from one humidity level to the next were strategically selected. The transition steps were 5% from 95% to 70% rH and 2% from 70% to the lowest rH limit (Table 3). The samples used in this study were produced from the same crystallization experiment and were introduced into the chamber sequentially for XRPD measurements. Measurements were repeated on fresh samples in order to verify the reproducibility of the results.

Table 3. Data collection parameters of in situ XRPD measurements upon controlled rH variation.

Cycle	Initial rH Levels (%)	Final rH Levels (%)	Step (% rH)	Temperature (K)	Waiting Time	Scans/Level
1	95	70	5	294.15	60 min	10
	70	60	2	294.15	60 min	10
2	95	70	5	294.15	60 min	10
	70	40	2	294.15	60 min	10
3	95	70	5	294.15	60 min	10
	70	30	2	294.15	60 min	10

In order to investigate the effect of temperature variation on octreotides at distinct rH levels, 6 subsequent cycles of XRPD data collection were performed. In these cycles, the sample underwent an increase/decrease in temperature from 294.15 K to 318.15 K. This was conducted for six selected humidity levels: 95%, 85%, 75%, 65%, 55%, and 45%. Intermediate waiting times of 60 min followed each transition from one humidity level to the next (Table 4).

Table 4. Data collection parameters of in situ XRPD measurements upon temperature variation at selected rH levels.

Cycle	Initial Temperature (K)	Final Temperature (K)	Step (K)	rH Level (%)	Waiting Time	Scans/Level
1	294.15	318.15	4	95	60 min	10
2	294.15	318.15	4	85	60 min	10
3	294.15	318.15	4	75	60 min	10
4	294.15	318.15	4	65	60 min	10
5	294.15	318.15	4	55	60 min	10
6	294.15	318.15	4	45	60 min	10

Finally, all XRPD profiles were analyzed using the Pawley method [38] implemented in the software HighScore Plus [37] in order to obtain refined values of the unit-cell parameters and to characterize the peak shape and background coefficients.

4. Discussion

The integration of a controlled humidity and temperature chamber into the laboratory X-ray diffraction system has significantly enhanced our capacity to investigate the impact of environmental conditions on biomacromolecular polycrystalline specimens. In this study, our primary objective was to evaluate the resilience of the pharmaceutical peptide octreotide under varying environmental conditions, spanning temperatures from 294.15 K to 318.15 K and rH levels from 95% to 30%. Despite notable variations in lattice parameters, the orthorhombic symmetry of the octreotide remained unaltered throughout these measurements. Moreover, the peptide's crystalline structure was retained, demonstrating its ability to revert to its initial state upon rehydration. These findings not only highlight the robustness of our controlled methodology in assessing the impact of environmental fluctuations on pharmaceutical peptides but also establish a novel threshold for humidity change tolerance, contrasting previous studies indicating crystallinity loss at 60% rH [6,39].

Furthermore, the observed stability of the octreotide peptide holds promise for advancing the development of more effective medications targeting severe medical conditions such as cancerous syndromes and acromegaly. This investigation serves as a catalyst for further exploration into the potential formulation of microcrystalline pharmaceuticals, leveraging their inherent stability and physicochemical attributes. The reliability and precision of data obtained via laboratory diffraction systems underscore the efficacy of XRPD as a technique for monitoring the crystalline characteristics of macromolecular pharmaceuticals, including peptide and protein-based drugs. The scalability of this methodology to an industrial level could optimize production processes and storage conditions, thereby expediting quality control measures for pharmaceutical products and enhancing the ADME profile of drugs [40,41].

Moreover, the increasing prominence of peptides as active pharmaceutical ingredients (APIs) underscores their diverse biological activities and therapeutic applications [42]. Incorporating peptides and proteins into pharmaceutical formulations offers advantages such as high target specificity, low toxicity, and precise modulation of biological pathways [43,44]. These biomolecules also exhibit lower immunogenicity compared to small-molecule drugs and can serve as scaffolds for designing novel therapeutic agents with enhanced efficacy and selectivity [45,46]. However, despite their promising properties, the storage of peptides and proteins poses significant challenges, including susceptibility to degradation, aggregation, and denaturation under various storage conditions such as temperature fluctuations, pH changes, humidity, and light exposure [47,48].

To address these challenges, the utilization of crystalline suspensions emerges as a promising strategy to enhance the pharmacokinetic properties of peptide-based pharma-

ceuticals. Crystalline suspensions offer improved stability, solubility, and bioavailability compared to amorphous formulations. Furthermore, controlled crystallization techniques can optimize ADME profiles [49,50]. Overall, these findings highlight the potential of in situ studies with humidity chambers in conjunction with XRPD not only in structure-based drug design but also in meeting the criteria for drug stability outlined by global regulatory bodies such as the International Council for Harmonization of Technical Requirements for Pharmaceuticals for Human Use (ICH) [39] and the Food and Drug Administration (FDA [51].

Relative humidity is crucial in pharmaceutical manufacturing processes and packaging, influencing the efficacy and stability of drugs. Low rH in a production line may desiccate drugs, while excessively high rH levels may promote microbial growth. Stress testing, which includes evaluation of the effects of temperature, humidity, oxidation, and photolysis on drug substances, is a standard process in pharmaceutical development. Understanding the behavior of pharmaceutical compounds under varying humidity conditions is crucial for ensuring product stability and efficacy.

Given the potential impact of unexpected humidity fluctuations on pharmaceutical products, particularly on their absorption characteristics from their ADME profiles, the findings from rH experiments can provide valuable insights into product behavior and stability. These insights are essential for optimizing production and post-production processes to maintain the physicochemical and biochemical characteristics of drugs, with a primary focus on their absorption profiles within the body. By understanding how humidity variations affect the absorption of drugs, pharmaceutical companies can better design formulations to ensure consistent and predictable absorption kinetics, ultimately optimizing the drug's therapeutic efficacy.

While XRPD serves as a robust method for monitoring the crystalline properties of peptides as octreotides, it is essential to acknowledge its limitations in discerning molecular degradation mechanisms comprehensively. To address this aspect, investigations usually integrate complementary analytical methods such as Fourier-transform infrared spectroscopy (FTIR) [52,53], high-performance liquid chromatography (HPLC) [54], and mass spectrometry (MS) [55,56], as previously utilized in peptide studies. These techniques offer complementary information on molecular conformational changes, chemical stability, and degradation products, thereby enhancing our understanding of peptide stability and degradation pathways.

The duration and temperature range of our study were designed to provide insights into the immediate structural responses of the microcrystalline specimen to humidity and temperature variations, simulating conditions relevant to accelerated stability testing. However, it is acknowledged that the condensed timeframe and maximum temperature of 318.15K (45 °C) may not encompass the full spectrum of long-term stability assessments recommended by regulatory guidelines. Future research may extend the present study duration to encompass longer-term stability evaluations, aligning more closely with ICH-compliant protocols [57]. This extension would provide a comprehensive understanding of octreotide's stability profile over extended periods and address concerns regarding potential degradation influences associated with shorter study durations and elevated temperatures.

Finally, further experiments are currently ongoing to enhance the resolution limits of collected XRPD profiles and verify the reproducibility of observations. Towards this goal, the exceptionally significant improvement in the quality of synchrotron XRPD data following the upgrade of ESRF to a fourth-generation circular accelerator, along with the utilization of a new data processing algorithm at beamline ID22, creates new expectations for more efficient analysis of XRPD diffraction data and for more precise structure determination with enhanced atomic resolution [35]. These measurements will contribute to the identification of optimal dehydration protocols and provide a deeper understanding of the structural changes induced by humidity variations, ultimately advancing pharmaceutical research and development efforts.

In summary, the experimental approach presented herein lays the groundwork for standardizing investigations into the structural changes of primary polycrystalline samples under varying humidity and temperature conditions, offering insights into crucial biological phenomena.

5. Conclusions

The exceptional stability exhibited by the pharmaceutical peptide octreotide across diverse humidity and temperature conditions presents promising avenues for drug optimization in treating severe diseases. These findings contribute to the understanding of pharmaceutical formulations and underscore the potential of leveraging their unique stability and biochemical/physicochemical properties for therapeutic purposes. Additionally, the utilization of high-quality data from X-ray diffraction laboratory diffractometers enhances the credibility of the XRPD method for in situ assessment of macromolecular crystals, establishing a recognized practice for studying structural changes during variations in environmental conditions.

The successful crystallization of octreotide has yielded a highly pure and stable crystalline material suitable for further characterization studies. High crystal yield and adequate precipitate are critical for conducting a series of XRPD measurements, facilitating the determination of crystal properties and their response to environmental factors. XRPD emerges as a powerful technique for in situ studies of crystalline materials, providing real-time information on crystal structure and phase transitions under varying environmental conditions.

Utilizing XRPD as a tool for product quality control ensures the consistency and reproducibility of pharmaceutical formulations by monitoring the crystallinity and structural integrity of APIs and excipients. This quality control process is vital for meeting regulatory standards and ensuring the efficacy, safety, and stability of pharmaceutical products. In conclusion, the integration of XRPD into pharmaceutical research and development practices holds promise for advancing drug optimization, formulation, and quality assurance processes, thereby contributing to the enhancement of healthcare outcomes and patient well-being.

References

1. Ducruix, A.; Giegé, R. (Eds.) *Crystallization of Nucleic Acids and Proteins: A Practical Approach*, 2nd ed.; Oxford University Press: Oxford, UK, 1999. [CrossRef]
2. Asherie, N. Protein crystallization and phase diagrams. *Methods* **2004**, *34*, 266–272. [CrossRef] [PubMed]
3. Govada, L.; Chayen, N.E. Choosing the Method of Crystallization to Obtain Optimal Results. *Crystals* **2019**, *9*, 106. [CrossRef]
4. Hageman, M.J. The Role of Moisture in Protein Stability. *Drug Dev. Ind. Pharm.* **1988**, *14*, 2047–2070. [CrossRef]
5. Hudaverdyan, T.G.; Kachalova, G.S.; Bartunik, H.D. Estimation of the effect of relative humidity on protein crystallization. *Crystallogr. Rep.* **2006**, *51*, 519–524. [CrossRef]
6. Zellnitz, S.; Narygina, O.; Resch, C.; Schroettner, H.; Urbanetz, N.A. Crystallization speed of salbutamol as a function of relative humidity and temperature. *Int. J. Pharm.* **2015**, *489*, 170–176. [CrossRef] [PubMed]
7. Rosenberger, F.; Howard, S.; Sowers, J.; Nyce, T. Temperature dependence of protein solubility—Determination and application to crystallization in X-ray capillaries. *J. Cryst. Growth* **1993**, *129*, 1–12. [CrossRef]
8. Budayova-Spano, M.; Dauvergne, F.; Audiffren, M.; Bactivelane, T.; Cusack, S. A methodology and an instrument for the temperature-controlled optimization of crystal growth. *Acta Crystallogr. Sect. D Struct. Biol.* **2007**, *63*, 339–347. [CrossRef] [PubMed]
9. Norrman, M.; Ståhl, K.; Schluckebier, G.; Al-Karadaghi, S. Characterization of insulin microcrystals using powder diffraction and multivariate data analysis. *J. Appl. Crystallogr.* **2006**, *39*, 391–400. [CrossRef]
10. Margiolaki, I.; Wright, J.P. Powder crystallography on macromolecules. *Acta Crystallogr. Sect. A Found. Crystallogr.* **2008**, *64*, 169–180. [CrossRef]
11. Karavassili, F.; Valmas, A.; Fili, S.; Georgiou, C.D.; Margiolaki, I. In Quest for Improved Drugs against Diabetes: The Added Value of X-ray Powder Diffraction Methods. *Biomolecules* **2017**, *7*, 63. [CrossRef]
12. Margiolaki, I. Macromolecular Powder Diffraction. In 2019. pp. 718–736. Available online: http://xrpp.iucr.org/cgi-bin/itr?url_ver=Z39.88-2003&rft_dat=what=chapter&volid=Ha&chnumo=7o1&chvers=v0001 (accessed on 11 October 2011).
13. Spiliopoulou, M.; Triandafillidis, D.-P.; Valmas, A.; Kosinas, C.; Fitch, A.N.; Von Dreele, R.B.; Margiolaki, I. Rietveld Refinement for Macromolecular Powder Diffraction. *Cryst. Growth Des.* **2020**, *20*, 8101–8123. [CrossRef]
14. Triandafillidis, D.P.; Karavassili, F.; Spiliopoulou, M.; Valmas, A.; Athanasiadou, M.; Nikolaras, G.; Fili, S.; Kontou, P.; Bowler, M.W.; Chasapis, C.T.; et al. The T_2 structure of polycrystalline cubic human insulin. *Acta Crystallogr. Sect. D Struct. Biol.* **2023**, *79*, 374–386. [CrossRef]
15. Rupley, J.A.; Careri, G. Protein Hydration and Function. In *Advances in Protein Chemistry*; Elsevier: Amsterdam, The Netherlands, 1991; pp. 37–172. [CrossRef] [PubMed]
16. Fenimore, P.W.; Frauenfelder, H.; McMahon, B.H.; Young, R.D. Bulk-solvent and hydration-shell fluctuations, similar to α- and β-fluctuations in glasses, control protein motions and functions. *Proc. Natl. Acad. Sci. USA* **2004**, *101*, 14408–14413. [CrossRef] [PubMed]
17. Atakisi, H.; Moreau, D.W.; Thorne, R.E. Effects of protein-crystal hydration and temperature on side-chain conformational heterogeneity in monoclinic lysozyme crystals. *Acta Crystallogr. Sect. D Struct. Biol.* **2018**, *74*, 264–278. [CrossRef]
18. Trampari, S.; Valmas, A.; Logotheti, S.; Saslis, S.; Fili, S.; Spiliopoulou, M.; Beckers, D.; Degen, T.; Nenert, G.; Fitch, A.N.; et al. *In situ* detection of a novel lysozyme monoclinic crystal form upon controlled relative humidity variation. *J. Appl. Crystallogr.* **2018**, *51*, 1671–1683. [CrossRef]
19. Logotheti, S.; Valmas, A.; Trampari, S.; Fili, S.; Saslis, S.; Spiliopoulou, M.; Beckers, D.; Degen, T.; Nénert, G.; Fitch, A.N.; et al. Unit-cell response of tetragonal hen egg white lysozyme upon controlled relative humidity variation. *J. Appl. Crystallogr.* **2019**, *52*, 816–827. [CrossRef]
20. Wang, L.; Wang, N.; Zhang, W.; Cheng, X.; Yan, Z.; Shao, G.; Wang, X.; Wang, R.; Fu, C. Therapeutic peptides: Current applications and future directions. *Signal Transduct. Target. Ther.* **2022**, *7*, 48. [CrossRef]
21. Spiliopoulou, M.; Karavassili, F.; Triandafillidis, D.-P.; Valmas, A.; Fili, S.; Kosinas, C.; Barlos, K.; Barlos, K.K.; Morin, M.; Reinle-Schmitt, M.L.; et al. New perspectives in macromolecular powder diffraction using single-photon-counting strip detectors: High-resolution structure of the pharmaceutical peptide octreotide. *Acta Crystallogr. Sect. A Found. Adv.* **2021**, *77*, 186–195. [CrossRef] [PubMed]
22. Pohl, E.; Heine, A.; Sheldrick, G.M.; Dauter, Z.; Schneider, T.; Wilson, K.S.; Kallen, J. Comparison of different X-ray data-collection systems using the crystal structure of octreotide. *Acta Crystallogr. Sect. D Struct. Biol.* **1995**, *51*, 60–68. [CrossRef]
23. Fili, S.; Valmas, A.; Spiliopoulou, M.; Kontou, P.; Fitch, A.; Beckers, D.; Degen, T.; Barlos, K.; Barlos, K.K.; Karavassili, F.; et al. Revisiting the structure of a synthetic somatostatin analogue for peptide drug design. *Acta Crystallogr. Sect. B Struct. Sci.* **2019**, *75*, 611–620. [CrossRef]
24. European Medicines Agency. Assessment Report Mycapssa International Non-Proprietary Name: Octreotide Procedure No. EMEA/H/C/005826/0000. Available online: https://www.ema.europa.eu/en/documents/assessment-report/mycapssa-epar-public-assessment-report_en.pdf (accessed on 15 September 2022).
25. Kuntz, I.D. Structure-Based Strategies for Drug Design and Discovery. *Science* **1992**, *257*, 1078–1082. [CrossRef] [PubMed]
26. Debnath, D.; Cheriyath, P. Octreotide. In *StatPearls*; StatPearls Publishing: Treasure Island, FL, USA, 2024. Available online: http://www.ncbi.nlm.nih.gov/books/NBK544333/ (accessed on 26 April 2024).

27. Zhao, J.; Fu, H.; Yu, J.; Hong, W.; Tian, X.; Qi, J.; Sun, S.; Zhao, C.; Wu, C.; Xu, Z.; et al. Prospect of acromegaly therapy: Molecular mechanism of clinical drugs octreotide and paltusotine. *Nat. Commun.* **2023**, *14*, 962. [CrossRef]

28. Li, S.-C.; Martijn, C.; Cui, T.; Essaghir, A.; Luque, R.M.; Demoulin, J.-B.; Castaño, J.P.; Öberg, K.; Giandomenico, V. The Somatostatin Analogue Octreotide Inhibits Growth of Small Intestine Neuroendocrine Tumour Cells. *PLoS ONE* **2012**, *7*, e48411. [CrossRef]

29. Battershill, P.E.; Clissold, S.P. Octreotide: A Review of its Pharmacodynamic and Pharmacokinetic Properties, and Therapeutic Potential in Conditions Associated with Excessive Peptide Secretion. *Drugs* **1989**, *38*, 658–702. [CrossRef]

30. Di, L. Strategic Approaches to Optimizing Peptide ADME Properties. *AAPS J.* **2015**, *17*, 134–143. [CrossRef]

31. Harris, A.G. Somatostatin and somatostatin analogues: Pharmacokinetics and pharmacodynamic effects. *Gut* **1994**, *35* (Suppl. S3), S1–S4. [CrossRef]

32. Han, B.; Tang, H.; Liang, Q.; Zhu, M.; Xie, Y.; Chen, J.; Li, Q.; Jia, J.; Li, Y.; Ren, Z.; et al. Preparation of long-acting microspheres loaded with octreotide for the treatment of portal hypertensive. *Drug Deliv.* **2021**, *28*, 719–732. [CrossRef] [PubMed]

33. Li, X.; Rao, T.; Xu, Y.; Hu, K.; Zhu, Z.; Li, H.; Kang, D.; Shao, Y.; Shen, B.; Yin, X.; et al. Pharmacokinetic and pharmacodynamic evidence for developing an oral formulation of octreotide against gastric mucosal injury. *Acta Pharmacol. Sin.* **2018**, *39*, 1373–1385. [CrossRef] [PubMed]

34. Tiberg, F.; Roberts, J.; Cervin, C.; Johnsson, M.; Sarp, S.; Tripathi, A.P.; Linden, M. Octreotide s.c. depot provides sustained octreotide bioavailability and similar IGF-1 suppression to octreotide LAR in healthy volunteers. *Br. J. Clin. Pharmacol.* **2015**, *80*, 460–472. [CrossRef]

35. Fitch, A.; Dejoie, C.; Covacci, E.; Confalonieri, G.; Grendal, O.; Claustre, L.; Guillou, P.; Kieffer, J.; de Nolf, W.; Petitdemange, S.; et al. ID22—The high-resolution powder-diffraction beamline at ESRF. *J. Synchrotron Radiat.* **2023**, *30*, 1003–1012. [CrossRef]

36. Basso, S.; Fitch, A.N.; Fox, G.C.; Margiolaki, I.; Wright, J.P. High-throughput phase-diagram mapping via powder diffraction: A case study of HEWL versus pH. *Acta Crystallogr. D Biol. Crystallogr.* **2005**, *61*, 1612–1625. [CrossRef] [PubMed]

37. Degen, T.; Sadki, M.; Bron, E.; König, U.; Nénert, G. The HighScore suite. *Powder Diffr.* **2014**, *29*, S13–S18. [CrossRef]

38. Pawley, G.S. Unit-cell refinement from powder diffraction scans. *J. Appl. Crystallogr.* **1981**, *14*, 357–361. [CrossRef]

39. Abraham, J. International Conference on Harmonisation of Technical Requirements for Registration of Pharmaceuticals for Human Use. In *Handbook of Transnational Economic Governance Regimes*; Tietje, C., Brouder, A., Eds.; Brill | Nijhoff: Leiden, The Netherlands, 2010; pp. 1041–1053. Available online: https://brill.com/view/book/edcoll/9789004181564/Bej.9789004163300.i-1081_085.xml (accessed on 27 November 2023).

40. Lipinski, C.A.; Lombardo, F.; Dominy, B.W.; Feeney, P.J. Experimental and computational approaches to estimate solubility and permeability in drug discovery and development settings. *Adv. Drug Deliv. Rev.* **1997**, *23*, 3–25. [CrossRef]

41. Prueksaritanont, T.; Tang, C. ADME of Biologics—What Have We Learned from Small Molecules? *AAPS J.* **2012**, *14*, 410–419. [CrossRef] [PubMed]

42. Kumar, V.; Bansal, V.; Madhavan, A.; Kumar, M.; Sindhu, R.; Awasthi, M.K.; Binod, P.; Saran, S. Active pharmaceutical ingredient (API) chemicals: A critical review of current biotechnological approaches. *Bioengineered* **2022**, *13*, 4309–4327. [CrossRef]

43. Lau, J.L.; Dunn, M.K. Therapeutic peptides: Historical perspectives, current development trends, and future directions. *Bioorganic. Med. Chem.* **2018**, *26*, 2700–2707. [CrossRef]

44. Bashir, S.; Fitaihi, R.; Abdelhakim, H.E. Advances in formulation and manufacturing strategies for the delivery of therapeutic proteins and peptides in orally disintegrating dosage forms. *Eur. J. Pharm. Sci.* **2023**, *182*, 106374. [CrossRef] [PubMed]

45. Fosgerau, K.; Hoffmann, T. Peptide therapeutics: Current status and future directions. *Drug Discov. Today* **2015**, *20*, 122–128. [CrossRef]

46. Muheem, A.; Shakeel, F.; Jahangir, M.A.; Anwar, M.; Mallick, N.; Jain, G.K.; Warsi, M.H.; Ahmad, F.J. A review on the strategies for oral delivery of proteins and peptides and their clinical perspectives. *Saudi Pharm. J.* **2016**, *24*, 413–428. [CrossRef]

47. Manning, M.C.; Chou, D.K.; Murphy, B.M.; Payne, R.W.; Katayama, D.S. Stability of Protein Pharmaceuticals: An Update. *Pharm. Res.* **2010**, *27*, 544–575. [CrossRef] [PubMed]

48. Nugrahadi, P.P.; Hinrichs, W.L.J.; Frijlink, H.W.; Schöneich, C.; Avanti, C. Designing Formulation Strategies for Enhanced Stability of Therapeutic Peptides in Aqueous Solutions: A Review. *Pharmaceutics* **2023**, *15*, 935. [CrossRef] [PubMed]

49. Mirza, S.; Miroshnyk, I.; Heinämäki, J.; Antikainen, O.; Rantanen, J.; Vuorela, P.; Vuorela, H.; Yliruusi, J. Crystal Morphology Engineering of Pharmaceutical Solids: Tabletting Performance Enhancement. *Aaps Pharmscitech* **2009**, *10*, 113–119. [CrossRef] [PubMed]

50. Khadka, P.; Ro, J.; Kim, H.; Kim, I.; Kim, J.T.; Kim, H.; Cho, J.M.; Yun, G.; Lee, J. Pharmaceutical particle technologies: An approach to improve drug solubility, dissolution and bioavailability. *Asian J. Pharm. Sci.* **2014**, *9*, 304–316. [CrossRef]

51. U.S. Department of Health and Human Services, Food and Drug Administration, Center for Veterinary Medicine (CVM). Guidance for Industry #5—Drug Stability Guidelines. 2008. Available online: https://www.fda.gov/media/69957/download (accessed on 1 November 2023).

52. Daéid, N.N. Forensic Sciences | Systematic Drug Identification. In *Encyclopedia of Analytical Science*; Elsevier: Amsterdam, The Netherlands, 2005; pp. 471–480. Available online: https://linkinghub.elsevier.com/retrieve/pii/B0123693977001977 (accessed on 26 April 2024).

53. Li, P.; Ford, L.; Haque, S.; McInerney, M.P.; Williams, H.D.; Scammells, P.J.; Thompson, P.E.; Jannin, V.; Porter, C.J.H.; Benameur, H.; et al. Lipophilic Salts and Lipid-Based Formulations: Enhancing the Oral Delivery of Octreotide. *Pharm. Res.* **2021**, *38*, 1125–1137. [CrossRef] [PubMed]

54. Yasin, M.S.; Hussain, K.; Khan, K.-U.-R.; Waris, K.; Kamran, M.; Dilshad, R.; Abid, H.M.U.; Sohail, I.; Ahmad, S.; Dilshad, R.; et al. Development and validation of a reversed-phase hplc method for assay of the octapeptide octreotide in raw material and pharmaceutical dosage form. *J. Popul. Ther. Clin. Pharmacol.* **2024**, *31*, 1195–1203. Available online: https://jptcp.com/index.php/jptcp/article/view/4048 (accessed on 26 April 2024).

55. Ismaiel, O.A.; Zhang, T.; Jenkins, R.; Karnes, H.T. Determination of octreotide and assessment of matrix effects in human plasma using ultra high performance liquid chromatography–tandem mass spectrometry. *J. Chromatogr. B* **2011**, *879*, 2081–2088. [CrossRef]

56. Cui, L.; Yang, Z.; Li, M.; Wei, Z.; Fei, Q.; Huan, Y.; Li, H. Structural characterization of octreotide impurities by on-line electrochemistry-tandem mass spectrometry. *Int. J. Mass Spectrom.* **2019**, *435*, 18–25. [CrossRef]

57. International Council for Harmonisation of Technical Requirements for Pharmaceuticals for Human Use. ICH Quality Guidelines. Available online: https://www.ich.org/page/quality-guidelines (accessed on 1 November 2023).